ChemPubSoc Europe
DOI: 10.1002/chem.201904151
CHEMISTRY A European Journal Communication

Pi Interactions |Hot Paper|

Singly and Doubly Quinoxaline-Fused B^{III} Subporphyrins

Koki Kise and Atsuhiro Osuka*[a]

Abstract: *B*-Phenyl B^{III} subporphyrin-α-diones prepared in a three-step reaction sequence from the parent subporphyrin were condensed with 1,2-diaminobenzenes to give the corresponding quinoxaline-fused subporphyrins in variable yields. Quinoxaline-fused *B*-phenyl-5,10,15-triphenyl B^{III} subporphyrin was transformed to the corresponding subporphyrin-α-dione in the same three-step reaction sequence, which was then condensed with 1,2-diaminobenzene to give doubly quinoxaline-fused subporphyrin. These quinoxaline-fused subporphyrins exhibit redshifted absorption and fluorescence spectra compared with the parent one. A singly quinoxaline-fused subporphyrin bearing three *meso*-bis(4-dimethylaminophenyl)aminophenyl substituents shows blueshifted fluorescence in less polar solvent, which has been ascribed to emission associated with charge recombination of intramolecular charge transfer (CT) state.

Subporphyrinatoboron(III) (hereafter called as subporphyrin),[1–5] is the genuine ring-contracted porphyrin with 14π aromatic circuit consisting of three pyrroles and three bridging methine carbons. Since the first synthesis in 2006,[1a] the chemistry of subporphyrins has been extensively studied, showing their unique properties and reactivities. Different from *meso*-aryl-substituted porphyrins, most of *meso*-aryl substituents in subporphyrins can rotate rather freely, hence causing large substituent effects on the optical and electronic properties.[2,3e] Taking advantage of this feature, many interesting examples have been explored. β-Substituted subporphyrins have been also developed,[4] such as β-halogenated,[4a] β-nitrated,[4b] β-aminated,[4b] and β-sulfanylated subporphyrins.[4c,e] But there are only limited examples of β-π-extended subporphyrins and only tribenzosubporphines **1**[1a] and *meso*-triphenyl-tribenzosubporphyrins **2** were reported.[2a] Herein, we report the synthesis and properties of singly and doubly quinoxaline-fused subporphyrins as rare examples of β-π-extended subporphyrins (Scheme 1).

Quinoxaline-fused porphyrins **3** were one of the representative β-π-extended porphyrins, which were originally and extensively developed by Crossley and co-workers.[6] These fused porphyrins were synthesized by the condensation of porphyrin-α-diones with 1,2-diaminobenzenes and the easiness of these condensation reactions allowed various types of quinoxaline-fused porphyrins. As related examples, π-extended phthalocyanines were actively prepared by Sastre-Santos et al. by imine-formation reaction of diaminophthalocyanines with cyclohexane-1,2,3,4,5,6-hexaone.[7] Our recent synthesis of subporphyrin-α-diones encouraged us to examine the exploration of quinoxaline-fused subporphyrins.[8]

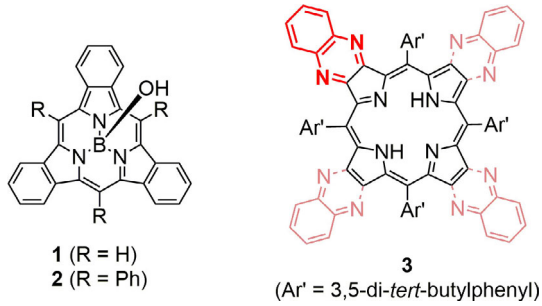

Scheme 1. β-π-Extended subporphyrins and quinoxaline-fused porphyrins.

The synthetic route to quinoxaline-fused subporphyrins is shown in Scheme 2. Subporphyrin-α-dione **5** was prepared by the reported procedure[8] in a three-step sequence from subporphyrin **4** and was reacted with 1,2-diaminobenzene **6** in a mixture of THF and MeOH (1:1) at 40 °C for four hours to give quinoxaline-fused subporphyrin **7** in 91 % yield. In the condensation reaction with **8**, the starting subporphyrin **5** was consumed at room temperature within 15 minutes, giving **9** in moderate yield of 42 %. The observed accelerated reaction for **9** may be attributed to high nucleophilicity of **8**. On the other hand, the reaction of **5** with **10** required longer reaction time

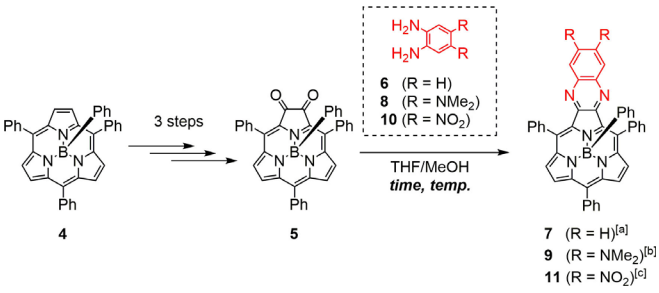

Scheme 2. Synthesis of monoquinoxalinosubporphyrins **7**, **9**, and **11**. Reaction conditions: [a] **5** (1.0 equiv), **6** (2.1 equiv), 40 °C, 4 h, 91 % yield. [b] **5** (1.0 equiv), **8** (1.2 equiv), room temperature, 15 min, 42 % yield. [c] **5** (1.0 equiv), **10** (1.2 equiv), 60 °C, 33 h, 15 % yield.

[a] K. Kise, Prof. Dr. A. Osuka
Department of Chemistry, Graduate School of Science
Kyoto University, Sakyo-ku, Kyoto 606-8502 (Japan)
E-mail: osuka@kuchem.kyoto-u.ac.jp

Supporting information and the ORCID identification number(s) for the author(s) of this article can be found under:
https://doi.org/10.1002/chem.201904151.

(33 h) and higher temperature (60 °C) to complete the conversion. This reaction afforded **11** in a poor yield of 15 %.

Next, we attempted to synthesize doubly quinoxaline-fused subporphyrin **15** (Scheme 3). Subporphyrin-α-dione **14** was prepared in the three-step sequence from **7** in a total yield of

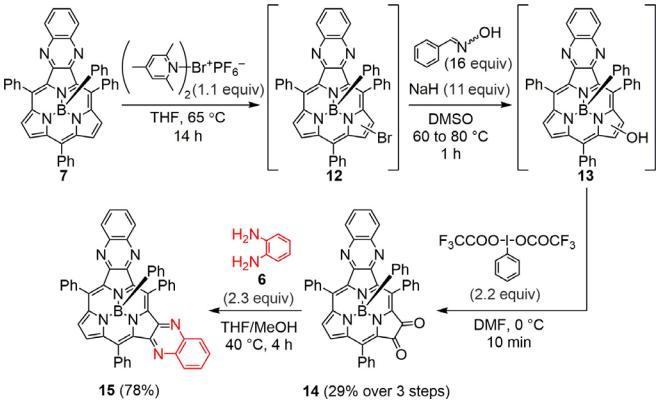

Scheme 3. Synthesis of bisquinoxalinosubporphyrin **15**.

29 %. Namely, **7** was brominated with bis(2,4,6-trimethylpyridine)bromonium hexafluorophosphate in refluxing THF to give a crude mixture containing β-monobrominated subporphyrin, β-dibrominated subporphyrin, and the starting material, which were difficult to separate. Then, this mixture was roughly purified through a silica-gel column and was reacted with benzaldehyde oxime in the presence of sodium hydride in DMSO at 60 °C for 30 min to give β-hydroxy subporphyrin **13** as a crude mixture. Then, this mixture dissolved in DMF was treated with [bis(trifluoroacetoxy)iodo]benzene (PIFA) at 0 °C, to furnish subporphyrin-α-dione **14**. Finally, **14** was condensed with 1,2-diaminobenzene **6** in a mixed solvent of THF and MeOH (1:1) at 40 °C, giving doubly quinoxaline-fused subporphyrin **15** in 78 % yield. The ^{1}H NMR spectrum of **15** in $CDCl_3$ shows a C_s-symmetric pattern, indicating the equivalence of both quinoxaline parts (Scheme 3).

Further, we attempted the synthesis of a quinoxaline-fused subporphyrin bearing electron-donating *meso*-aryl substituents, **21**, to examine whether the characteristic *p*-aminophenyl substituent effect is still active for the quinoxaline-fused substrate (Scheme 4).[2c] Similarly to the synthesis of **5** and **14**, subporphyrin-α-dione **19** was prepared in the three-step sequence from *B*-phenyl-5,10,15-tris(4-bromophenyl)subporphyrin **16** (see section 2.7–2.10 in Supporting Information for details). Then, **19** was reacted with 1,2-diaminobenzene **6** in a mixed solvent of THF and MeOH (1:1) at 40 °C for 4 h, affording **20** in good yield of 81 %. Finally, **20** was reacted with bis(4-dimethylaminophenyl)amine in the presence of tris(dibenzylideneacetone)dipalladium(0) (Pd_2dba_3), 2-dicyclohexylphosphino-2′,4′,6′-triisopropylbiphenyl (XPhos), and sodium *tert*-butoxide in toluene at 100 °C for 28 h. Subsequent separation by silica-gel column chromatography and recrystallization from CH_2Cl_2 and MeOH gave **21** in 54 % yield.

The structures of **7**, **9**, and **15** were unambiguously determined by X-ray diffraction analysis (Figure 1 and section 4 in

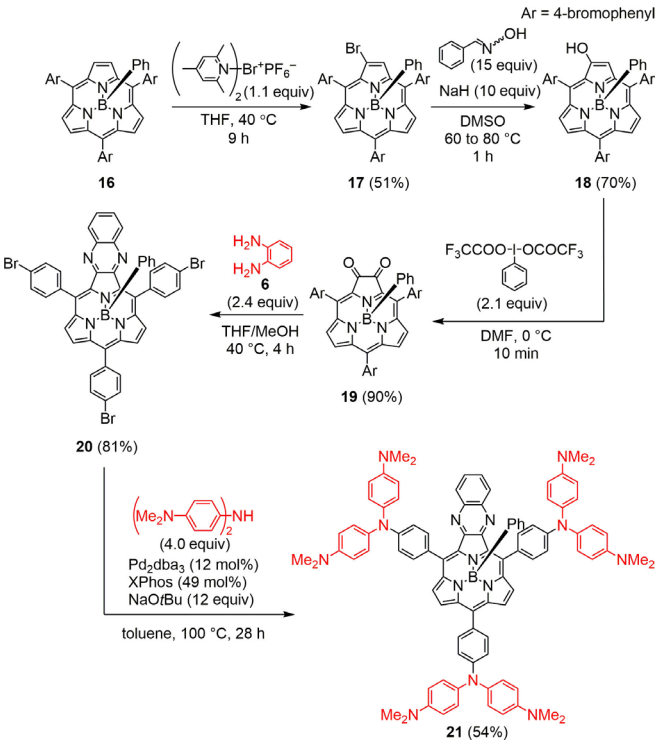

Scheme 4. Synthesis of *meso*-functionalized monoquinoxalinosubporphyrin **21**.

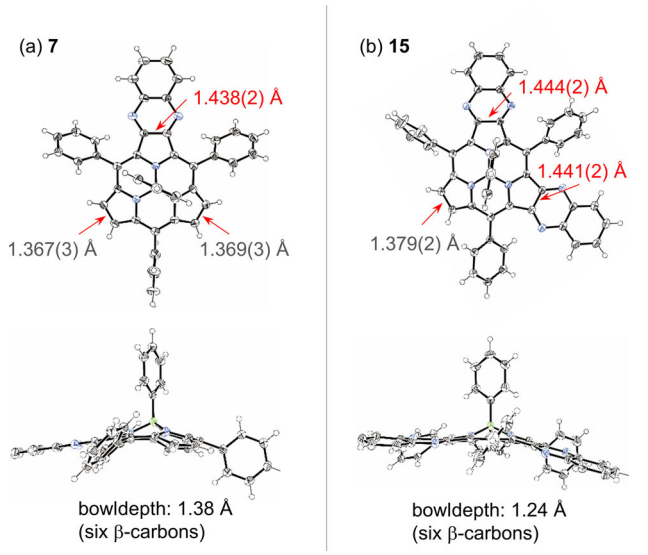

Figure 1. X-Ray crystal structures of (a) **7** and (b) **15**. Solvent molecules are omitted for clarity. The thermal ellipsoids are scaled at 50 % probability level.

the Supporting Information). The bowl depths are 1.38 Å for **7**, 1.33 Å for **9**, and 1.24 Å for **15**.[9] Characteristically, the β-β bond lengths at the fused side are significantly longer (1.438–1.444 Å) compared with those of non-fused sides (1.367–1.379 Å). This implies the increased single bond character of the β-β bonds at the fused side. On the other hand, the C(β)–N bond lengths in **7** and **15** (1.315–1.321 Å, Figure S4-2 in the Supporting Information) are close to that of C–N double bond (1.29 Å) rather than C–N single bond (1.47 Å), implying the sig-

nificant double bond character in C(β)–N bonds. Previously, these trends of bond lengths were theoretically predicted for oligo(quinoxaline-fused)porphyrins by Lü et al.[6a]

The absorption and fluorescence spectra of the quinoxaline-fused subporphyrins in CH_2Cl_2 are shown in Figure 2. Unlike the reference *B*-phenyl-5,10,15-triphenylsubporphyrin **4**, singly quinoxaline-fused subporphyrin **7** exhibits a split Soret-like band at 345 and 380 nm and Q-like bands at 500 and 539 nm, whereas doubly quinoxaline-fused subporphyrin **15** exhibits more complicated Soret-like and Q-like bands (Figure 2a). Fluorescence was observed at 613 nm for **7** and 609 nm for **15** with quantum yields of 0.044 and 0.060, respectively, which are smaller than that of **4** ($\Phi_F = 0.16$). Introduction of electron-donating (-NMe_2) or electron-withdrawing (-NO_2) substituents at the quinoxaline part resulted in the redshifts in Soret-like bands (Figure 2b). Especially, compound **11** displays a broad band reaching around 700 nm and is non-fluorescent in CH_2Cl_2. Although **7** and **20** show almost the similar UV/Vis absorption spectra, **21** exhibits a quite different panchromatic absorption spectrum up to around 750 nm. Interestingly, the fluorescence behavior of **21** is dependent sensitively on the solvent polarity, which is different from **4** and **7** (Figure S3–6-3-7 and Table S3-2 in the Supporting Information). Although practically non-fluorescent in CH_2Cl_2 ($\Phi_F < 0.001$), **21** showed a weak emission over 750 nm in toluene ($\Phi_F = 0.055$) and exhibited a slightly blueshifted emission at 737 nm with increased fluorescence quantum yield of 0.253 in a binary solvent (toluene/cyclohexane = 1:9) as summarized in Table 1. The results may be understood by considering the following mechanism. Franck–Condon excited state of **21** relaxes to an intramolecular charge-transfer state even in non-polar solvent systems, such as toluene and toluene/cyclohexane (1:9). This CT state emits fluorescence associated with charge recombination to regenerate the ground state in non-polar solvents, but does not emit fluorescence in polar solvents probably due to very rapid charge recombination. The energy level of the CT state is slightly higher in toluene/cyclohexane (1:9) than in toluene in agreement with the observed blue shift in the mixed solvent.

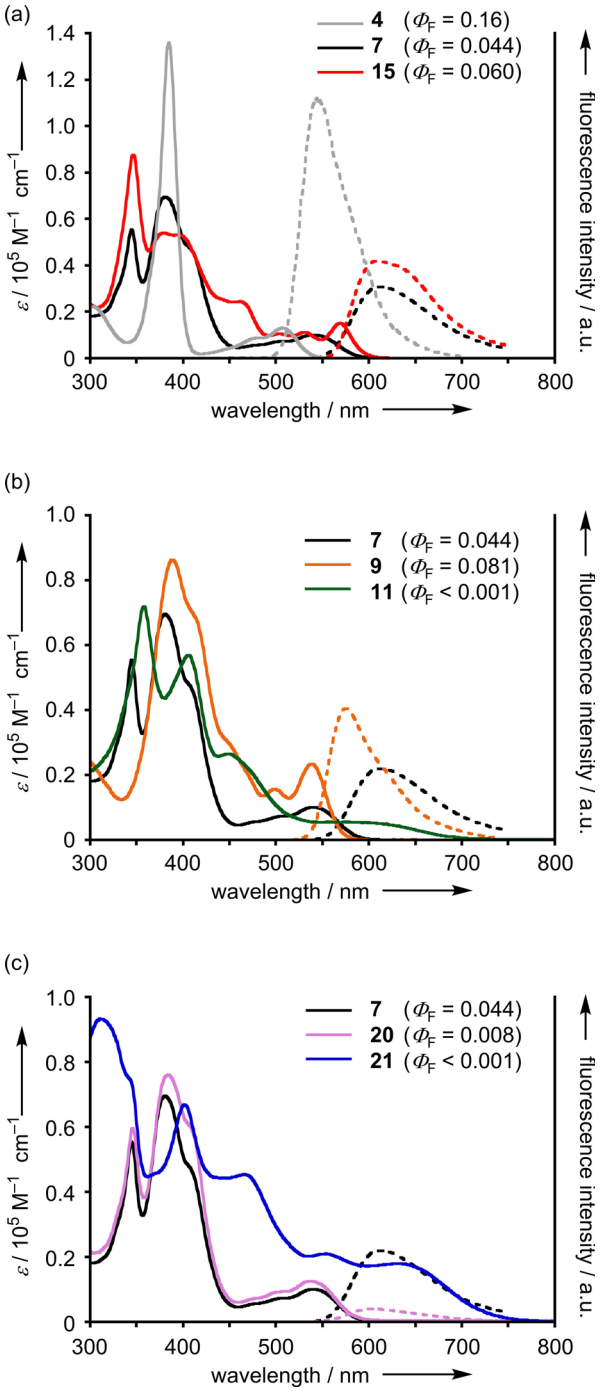

Figure 2. UV/Vis absorption (solid) and fluorescence (dashed) spectra of (a) **4** (gray), **7** (black), and **15** (red), (b) **7** (black), **9** (orange), and **11** (green), and (c) **7** (black), **20** (pink), and **21** (blue) in CH_2Cl_2.

Table 1. Summary of optical properties of quinoxalinosubporphyrins **4**, **7**, **9**, **15**, **20**, and **21** in CH_2Cl_2.

Compd.	Φ_F[a]	τ_F [ns][a]	k_r [s^{-1}]	k_{nr} [s^{-1}]	Stokes shift [cm^{-1}]
4	0.16	2.0	8.1×10^7	4.2×10^8	1240
7	0.044	1.8	2.4×10^7	5.2×10^8	2240
9	0.081	1.3	6.3×10^7	7.2×10^8	1210
15	0.060	2.3	2.6×10^7	4.0×10^8	1150
20	0.008	0.31	2.5×10^7	3.2×10^9	2060
21	< 0.001	–	–	–	–
21[b]	0.055	1.7	3.3×10^7	5.7×10^8	> 2510[c]
21[d]	0.253	4.2	6.1×10^7	1.8×10^8	2510

[a] Excited at Soret-like bands (see Figures S3-1 and S3–5 in the Supporting Information for detail). [b] In toluene. [c] Stokes shift was not exactly determined since the emission peak top was out of detection range. [d] In toluene/cyclohexane (1:9).

Density functional theory (DFT) calculations have been performed for quinoxaline-fused subporphyrins. Molecular orbital (MO) diagrams of **4**, **7**, **15**, and **21** are shown in Figure 3 (Figures S6-1–S6-3 in the Supporting Information). Compared with the reference subporphyrin **4**, singly quinoxaline-fused subporphyrin **7** possesses largely stabilized LUMO (−2.66 eV), which results in a diminished HOMO–LUMO gap of 2.79 eV. This is consistent with the redshifted absorption and fluorescence of **7**. Installation of fused quinoxaline unit continuously caused decrease in the energy level of a_2-like orbital and increase in

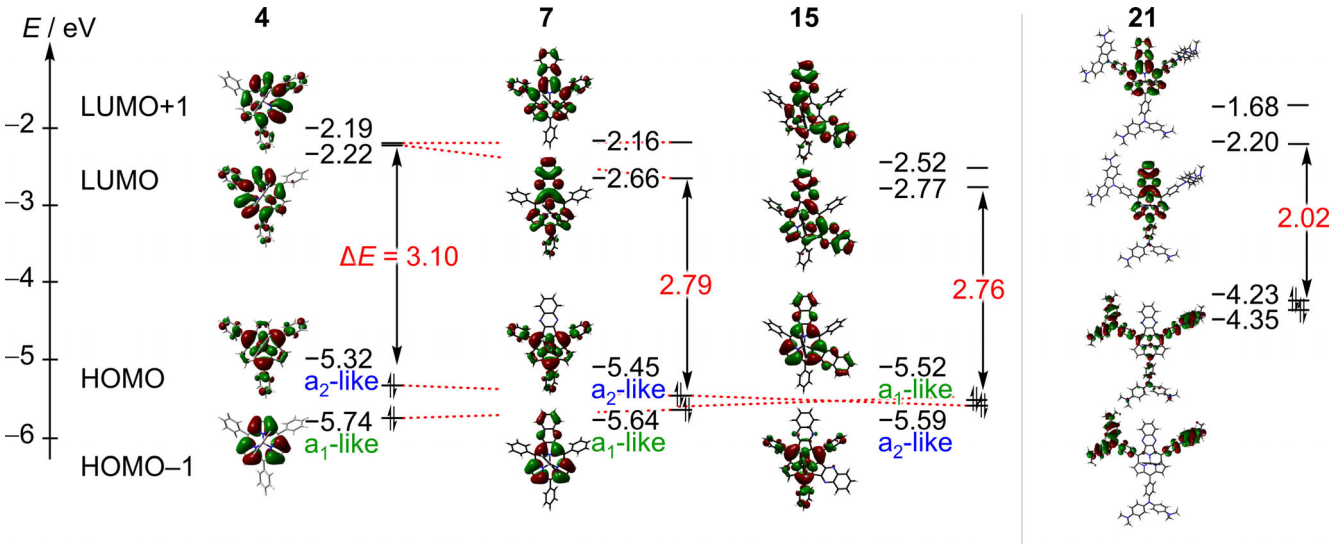

Figure 3. Molecular orbital diagrams of **4**, **7**, **15**, and **21** calculated at the level of B3LYP/6–311G(d).

the energy level of a_1-like orbital. As a result, HOMOs in **4** and **7** are a_2-like orbitals, but that in **15** is a_1-like orbital and HOMO–LUMO gap of **15** (2.76 eV) is almost similar to that of **7** (2.79 eV). These calculated results are consistent with the absorption and electrochemical data (see below). On the other hand, **21** showed largely destabilized HOMO (−4.23 eV), apparently due to the strong effect of the electron-donating *meso*-substituents. This explains the further redshift in absorption and fluorescence spectra. Especially, the calculated S_0–S_1 transition ($\lambda = 744$ nm) of **21** is mainly assigned to HOMO–LUMO transition, according to time-dependent (TD) DFT calculations (Figure S6-4 and Table S6-1–S6-6 in the Supporting Information). The calculation indicates that HOMO and LUMO in **21** are, respectively, localized in the *meso*-aryl groups and quinoxalinosubporphyrin moiety, implying intramolecular charge-transfer character.

Finally, electrochemical measurements were conducted. The first oxidation and reduction potentials, electrochemical HOMO–LUMO gaps, and theoretically calculated HOMO–LUMO gaps are summarized in Table 2 (Table S5–1 in the Supporting Information for detail). Electrochemical HOMO–LUMO gaps ($E_{ox.1}-E_{red.1}$) were correlated well with theoretically calculated energy gaps with correlation coefficient (R^2) of 0.940 (Figure S5-2 in the Supporting Information).

In summary, rare β-π-extended subporphyrin, namely, singly and doubly quinoxaline-fused subporphyrins, were synthesized by the double condensation of subporphyrin-α-diones with 1,2-diaminobenzenes. Introduction of electron-donating amino groups in *meso*-aryl substituents gave push-pull type subporphyrin **21** with redshifted absorption and solvent-sensitive fluorescence from intramolecular CT state. The subporphyrin **21** can be regarded as the first example of subporphyrin functionalized simultaneously at *meso*- and β-positions, revealing that electronic properties can also be tuned effectively by modifying *meso*-aryl substituents in β-π-extended subporphyrin.

Table 2. First oxidation and reduction potentials, electrochemical HOMO–LUMO gaps, and theoretically calculated HOMO–LUMO gaps of **7**, **9**, **11**, **15**, **20**, and **21**.

Compd.	$E_{ox.1}$ [V]	$E_{red.1}$ [V]	$E_{ox.1}-E_{red.1}$ [eV]	$E_{LUMO}-E_{HOMO}$ [eV][c]
7	0.72[a]	−1.76[b]	2.48	2.79
9	0.46[b]	−1.92[b]	2.38	2.86
11	0.82[a]	−1.07[a]	1.89	2.47
15	0.77[a]	−1.66[b]	2.43	2.76
20	0.80[a]	−1.53[b]	2.33	2.79
21	−0.23[a]	−1.77[a]	1.54	2.02

[a] Determined by cyclic voltammetry. [b] Determined by differential pulse voltammetry. [c] Calculated at B3LYP/6–311G(d) level.

Acknowledgements

This work was supported by JSPS KAKENHI of Scientific Research (A; 18H03910) and Challenging Exploratory Research (18K19074). K.K. acknowledges JSPS fellowship for young scientists.

Conflict of interest

The authors declare no conflict of interest.

Keywords: fused structures · push-pull systems · quinoxalines · subporphyrins · pi extensions

[1] a) Y. Inokuma, J. H. Kwon, T. K. Ahn, M.-C. Yoo, D. Kim, A. Osuka, *Angew. Chem. Int. Ed.* **2006**, *45*, 961; *Angew. Chem.* **2006**, *118*, 975; b) T. Torres, *Angew. Chem. Int. Ed.* **2006**, *45*, 2834; *Angew. Chem.* **2006**, *118*, 2900; c) R. Myśliborski, L. Latos-Grażyński, L. Szterenberg, T. Lis, *Angew. Chem. Int. Ed.* **2006**, *45*, 3670; *Angew. Chem.* **2006**, *118*, 3752; d) A. Osuka, E. Tsurumaki, T. Tanaka, *Bull. Chem. Soc. Jpn.* **2011**, *84*, 679; e) C. G. Claessens, D. González-Rodríguez, M. S. Rodríguez-Morgade, A. Medina, T. Torres, *Chem. Rev.* **2014**, *114*, 2192; f) S. Shimizu, *Chem. Rev.* **2017**, *117*, 2730.

[2] a) E. A. Makarova, S. Shimizu, A. Matsuda, E. A. Luk'yanets, N. Kobayashi, *Chem. Commun.* **2008**, 2109; b) Y. Inokuma, S. Easwaramoorthi, S. Y. Jang, K. S. Kim, D. Kim, A. Osuka, *Angew. Chem. Int. Ed.* **2008**, *47*, 4840; *Angew. Chem.* **2008**, *120*, 4918; c) Y. Inokuma, S. Easwaramoorthi, Z. S. Yoon, D. Kim, A. Osuka, *J. Am. Chem. Soc.* **2008**, *130*, 12234; d) S.-y. Hayashi, Y. Inokuma, A. Osuka, *Org. Lett.* **2010**, *12*, 4148; e) H. Sugimoto, M. Muto, T. Tanaka, A. Osuka, *Eur. J. Org. Chem.* **2011**, 71.

[3] a) M. Kitano, S.-y. Hayashi, T. Tanaka, H. Yorimitsu, N. Aratani, A. Osuka, *Angew. Chem. Int. Ed.* **2012**, *51*, 5593; *Angew. Chem.* **2012**, *124*, 5691; b) M. Kitano, S.-y. Hayashi, T. Tanaka, N. Aratani, A. Osuka, *Chem. Eur. J.* **2012**, *18*, 8929; c) M. Kitano, D. Shimizu, T. Tanaka, H. Yorimitsu, A. Osuka, *J. Porphyrins Phthalocyanines* **2014**, *18*, 659; d) D. Shimizu, H. Mori, M. Kitano, W.-Y. Cha, J. Oh, T. Tanaka, D. Kim, A. Osuka, *Chem. Eur. J.* **2014**, *20*, 16194; e) K. Kise, K. Yoshida, R. Kotani, D. Shimizu, A. Osuka, *Chem. Eur. J.* **2018**, *24*, 19136.

[4] a) E. Tsurumaki, Y. Inokuma, S. Easwaramoorthi, J. M. Lim, D. Kim, A. Osuka, *Chem. Eur. J.* **2009**, *15*, 237; b) E. Tsurumaki, A. Osuka, *Chem. Asian J.* **2013**, *8*, 3042; c) K. Yoshida, A. Osuka, *Chem. Asian J.* **2015**, *10*, 1526; d) M. Kitano, Y. Okuda, E. Tsurumaki, T. Tanaka, H. Yorimitsu, A. Osuka, *Angew. Chem. Int. Ed.* **2015**, *54*, 9275; *Angew. Chem.* **2015**, *127*, 9407; e) K. Yoshida, A. Osuka, *Chem. Eur. J.* **2016**, *22*, 9396.

[5] a) S. Shimizu, A. Matsuda, N. Kobayashi, *Inorg. Chem.* **2009**, *48*, 7885; b) S. Saga, S.-y. Hayashi, K. Yoshida, E. Tsurumaki, P. Kim, Y. M. Sung, J. Sung, T. Tanaka, D. Kim, A. Osuka, *Chem. Eur. J.* **2013**, *19*, 11158; c) E. Tsurumaki, J. Sung, D. Kim, A. Osuka, *J. Am. Chem. Soc.* **2015**, *137*, 1056; d) R. Kotani, K. Yoshida, E. Tsurumaki, A. Osuka, *Chem. Eur. J.* **2016**, *22*, 3320; e) E. Tsurumaki, J. Sung, D. Kim, A. Osuka, *Angew. Chem. Int. Ed.* **2016**, *55*, 2596; *Angew. Chem.* **2016**, *128*, 2642.

[6] a) T. X. Lü, J. R. Reimers, M. J. Crossley, N. S. Hush, *J. Phys. Chem.* **1994**, *98*, 11878; b) M. J. Crossley, L. J. Govenlock, J. K. Prashar, *J. Chem. Soc. Chem. Commun.* **1995**, 2379; c) J. R. Reimers, T. X. Lü, M. J. Crossley, N. S. Hush, *Chem. Phys. Lett.* **1996**, *256*, 353; d) K. Sendt, L. A. Johnston, W. A. Hough, M. J. Crossley, N. S. Hush, J. R. Reimers, *J. Am. Chem. Soc.* **2002**, *124*, 9299; e) M. J. Crossley, P. Thordarson, *Angew. Chem. Int. Ed.* **2002**, *41*, 1709; *Angew. Chem.* **2002**, *114*, 1785; f) M. J. Crossley, P. J. Sintic, J. A. Hutchison, K. P. Ghiggino, *Org. Biomol. Chem.* **2005**, *3*, 852; g) T. Khoury, M. J. Crossley, *Chem. Commun.* **2007**, 4851.

[7] a) V. M. Blas-Ferrando, J. Ortiz, J. Follana-Berná, F. Fernández-Lázaro, A. Campos, M. Mas-Torrent, Á. Sastre-Santos, *Org. Lett.* **2016**, *18*, 1466; b) J. Follana-Berná, D. Inan, V. M. Blas-Ferrando, N. Gorczak, J. Ortiz, F. Manjón, F. Fernández-Lázaro, F. C. Grozema, Á. Sastre-Santos, *J. Phys. Chem. C* **2016**, *120*, 26508; c) J. Follana-Berná, S. Seetharaman, L. Martín-Gomis, G. Charalambidis, A. Trapali, P. A. Karr, A. G. Coutsolelos, F. Fernández-Lázaro, F. D'Souza, Á. Sastre-Santos, *Phys. Chem. Chem. Phys.* **2018**, *20*, 7798; d) S. Seetharaman, J. Follana-Berná, L. Martín-Gomis, G. Charalambidis, A. Trapali, P. A. Karr, A. G. Coutsolelos, F. Fernández-Lázaro, Á. Sastre-Santos, F. D'Souza, *ChemPhysChem* **2019**, *20*, 163.

[8] K. Yoshida, W. Cha, D. Kim, A. Osuka, *Angew. Chem. Int. Ed.* **2017**, *56*, 2492; *Angew. Chem.* **2017**, *129*, 2532.

[9] Bowl depth is defined by the distance between the boron atom and the mean plane of the peripheral six β-carbons of subporphyrin macrocycle.

Manuscript received: September 9, 2019
Revised manuscript received: September 30, 2019
Version of record online: ■■ ▮▮, 0000

COMMUNICATION

Pi Interactions

*K. Kise, A. Osuka**

■■ – ■■

Singly and Doubly Quinoxaline-Fused B^{III} Subporphyrins

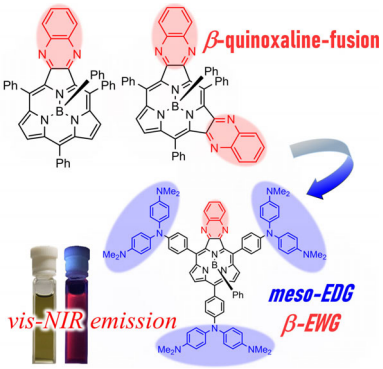

Push-pull systems: Singly and doubly quinoxaline-fused subporphyrins were synthesized by condensation of subporphyrin β,β-diketone with 1,2-diaminobenzenes. These fused subporphyrins exhibit redshifted absorption and fluorescence spectra. A singly quinoxaline-fused subporphyrin bearing three *meso*-bis(4-dimethylaminophenyl)aminophenyl substituents exhibits charge-recombination fluorescence of intramolecular CT state (see scheme).